#### MATERIALS PROCESSING AND KINETIC PHENOMENA: IN HONOR OF CARL V. THOMPSON

### Advances in Experimental Studies of Grain Growth in Thin Films

KATAYUN BARMAK  $^{\circ}$ ,  $^{1,4}$  JEFFREY M. RICKMAN  $^{\circ}$ , and MATTHEW J. PATRICK  $^{\circ}$ 

1.—Department of Applied Physics and Applied Mathematics, Columbia University, New York, NY 10027, USA. 2.—Department of Materials Science and Engineering, Lehigh University, Bethlehem, PA 18015, USA. 3.—Department of Physics, Lehigh University, Bethlehem, PA 18015, USA. 4.—e-mail: kb2612@columbia.edu

In this article, we review recent developments in the experimental study of grain growth in nanocrystalline metallic thin films, emphasizing transmission electron microscopy-based imaging and orientation mapping techniques and highlighting useful experimental and data analytical frameworks for dynamic experiments. Studies of grain growth have fallen short of the scale required to fully characterize the coarsening process, and models still fail to fully capture the true behavior of grain growth in polycrystalline systems as they pertain to geometric, topological and crystallographic metrics. Moreover, existing grain growth studies are either coarse in time and temperature or otherwise limited in scope. Nevertheless, important observations such as the stagnation of thin film grain growth at a universal grain size distribution and the strong correlations between the grain boundary character distributions in thin film and bulk materials motivate larger-scale dynamic studies. Additionally, recent hardware and software advances have removed bottlenecks to large-scale and in situ data acquisition via (1) automated grain boundary segmentation in micrographs, (2) low thermal mass microelectromechanical systems and (3) integrated hardware-software drift correction and data management solutions. We argue that these innovations render thin films a key integrated experimental platform for the next generation of grain growth studies.

#### INTRODUCTION

Due to their immense technological, scientific and engineering importance, polycrystalline thin film materials and, in particular, their microstructural evolution have been studied extensively. Grain size, grain morphology and grain boundary structure and motion characterize the mesoscale behavior of polycrystalline materials and dictate their associated macroscopic behavior, properties and performance, including their mechanical properties and failure modes, chemical resistance, mass transport characteristics, the propensity for phase transformations and electronic properties. While experimental observations of grain growth and microstructural evolution have yielded considerable insights into the coarsening process. 15–23 it is

fair to say that existing theories of grain growth and computer simulations fail to fully capture some salient aspects of microstructural development, <sup>24,25</sup> particularly as they pertain to topological features of the structure, such as grain-neighbor correlations. <sup>25</sup> In other words, scientists and engineers still lack the predictive, quantitative tools needed for realistic microstructural design and must therefore largely rely on trial and error to optimize microstructures.

This article addresses some recent advances made in experimental characterization of grain growth in nanocrystalline thin films and is structured as follows. We first summarize the problems associated with characterizing grain growth and present thin films as an attractive experimental platform for conducting dynamic coarsening studies (sections "Challenges in Characterizing Grain Growth", "Thin Films as an Experimental Platform for Grain Growth Studies"). We then describe transmission electron microscopy (TEM)-based techniques for

static characterization of grain growth, highlighting advances in image processing for high-throughput data analysis (sections "Static Imaging and Characterization") and key results obtained from scanning (S/)TEM-based orientation mapping of thin films, emphasizing grain boundary character and energy considerations as they pertain to microstructural evolution in thin films (sections "Static Orientation Mapping and Grain Boundary Character Distributions", "Thin Film Considerations for Grain Boundary Character Distribution"). Finally, we present developments and perspectives on in situ S/TEM-based studies of the dynamics of grain coarsening, including recent results and future directions for experiments and data analytical frameworks (sections "Information Technology and Instrumentation for In Situ TEM Experiments"— "Data Analytics and Model Integration of Dynamic Grain Growth Experiments").

### CHALLENGES IN CHARACTERIZING GRAIN GROWTH

Grain growth is governed by complex interactions among the ensemble of crystallites comprising the microstructure and their delimiting grain boundaries. The interactions, in turn, result in a wide array of energy reduction mechanisms, particularly in thin films. Each aspect of the microstructure can only be described in large parameter spaces, even when detailed atomic-scale structure is ignored. More specifically, a mesoscale description of microstructure comprises, in part, (1) strictly geometric and topological considerations (e.g., grain size distributions, number of nth nearest neighbors of grains, and integral mean curvature 24,26-28) and (2) crystallographic features (e.g., orientation texture and grain boundary character distribution (GBCD)<sup>29</sup>). Further complicating this description is the spectrum of anisotropic grain boundary energies associated with the boundary network and its role in governing coarsening behavior. 30,31 Finally, other factors (e.g., grain boundary pinning, grooving and drag) exemplify important interplays among the crystallographic and geometric aspects of the microstructure.  $^{15-17,32-37}$  As just one example of these interactions, crystallographic considerations are intricately related to certain geometric aspects of the network, especially near triple junctions. Conservation laws, for example, dictate the allowed boundary character distribution associated with a given triple junction, 39-41 while the interfacial energy associated with boundary character plays an important role in determining the dihedral angles of the junction.<sup>38</sup> Given these considerations, it is evident that designing integrated experiments for holistic characterization of grain growth is

Beyond experimental design, integrated analysis of coarsening presents daunting statistical challenges. For example, the acquisition of a grain size

distribution typically requires  $\sim 1000$  grains to draw conclusions within 5% uncertainty. 42 Moreover, a crystallographic enumeration of boundary geometries, even in coarse 10° binning of the fivedimensional GBCD, yields > 6500 macroscopic boundary characters for cubic crystals, and so statistically significant results require the characterization of  $> 10^4$  boundaries for a single sample. <sup>43,44</sup> As a result, when microstructural features are naively treated separately, experiments concerning grain growth offer incomplete information, as decoupling the effects of one microstructural aspect from another is often impossible. Instead, the keys to understanding coarsening lie in informed reductions of the problem-space and large-scale correlative and dynamic measurements. We note that dynamic experiments concerning grain growth are only now becoming feasible, but their results might allow researchers to mine cross-cutting datasets for relationships that further illuminate the grain growth process. This is as much a data science problem as it is one of materials physics, but large-scale data must first be acquired.

Grain growth is, irreducibly, a dynamic process, and ex situ characterization through static imaging and analysis only provides a piecemeal picture. Due to technological constraints, however, most currently available data concerning grain growth have been collected at relatively coarse time intervals and only recently has the examination of the same sample region before, during and after processing become practical. 45–49 Thus, it has been difficult to connect the various microstructural descriptors to the dynamic evolution of the system, despite their centrality to the problem. As a recent example of the importance of such dynamic studies, and the contradictory nature of the existing body of work, recent experiments on microcrystalline bulk materials have suggested that the previously well-accepted curvature-driven model of grain boundary migration is likely, at best, a partial description of the behavior of grain boundaries in polycrystals. 49 Nonetheless, recent computer simulations of grain growth have consistently shown curvature as an important consideration for grain growth. 25,28

### THIN FILMS AS AN EXPERIMENTAL PLATFORM FOR GRAIN GROWTH STUDIES

Nanocrystalline thin film materials offer an excellent experimental platform for studying the dynamics of the process of grain growth and grain boundary migration, and their structure makes them ideal candidates to address some of the issues summarized above. Thin film microstructures are especially amenable to in situ and correlative microscopy techniques in ways that bulk materials' structures are not. In particular, owing to a film's (straightforwardly achieved) columnar microstructure, where grains span the full thickness of the sample and boundaries are perpendicular to the

surfaces of the film, a strong approximation of the 3D structure is known a priori from 2D projections captured in transmission. Micrographs from the transmission electron microscope (TEM) therefore contain virtually complete direct-space information about the sample. Even in this limit, thin film microstructures act as a close proxy to bulk materials, <sup>47,50–53</sup> but microstructural interrogation can be accomplished while avoiding complications inherent to boundary network reconstruction in bulk materials. <sup>54</sup> Furthermore, direct TEM images can be captured rapidly and nondestructively using widely available instrumentation present at many institutions.

Precession enhanced electron diffraction (PED)based orientation mapping is also available in the S/TEM. 55-57 This technique offers the highest available spatial resolution for orientation mapping, typically  $\sim 1$  nm,<sup>58</sup> but comes at the cost of slow acquisition on the order of tens of minutes per field of view. PED also typically has an angular resolution limited to ≥ 0.5°, although recent work improving template matching for spot patterns has reduced this in some instances to  $< 0.2^{\circ}$ . Furthermore, by deconvolving overlapping patterns via multiindexing, in some instances deviations from columnarity in the grains can be resolved via through thickness information in the film where it is not fully columnar. 55 For more complex microstructures, 3D orientation mapping in the TEM has also been proposed and shown some recent success. 60-63

Employing thin films in conjunction with new technologies for in situ experiments permits nondestructive, dynamical characterization of both a region's local geometric and crystallographic structure non-destructively, without any change in instrumentation. More specifically, recent advances in microelectromechanical system (MEMS) chips and low thermal-drift TEM holders<sup>64</sup> coupled with computer vision for microstructural analysis 65 are enabling this next generation of in situ microstructural measurements in the TEM. This experimental workflow permits non-destructive, high time resolution direct-space imaging [∼1 frame per second (fps)] of grain growth during in situ heating experiments and intermittent PED-based orientation mapping, offering the possibility of characterization ofcomplete. one-stop microstructure during grain growth.

These advantages can be contrasted with difficulties associated with corresponding studies in the bulk. Non-destructive, dynamic characterization of bulk materials can still only be accomplished at relatively coarse intervals in time and space. For example, using a technique like scanning electron microscopy (SEM) or electron backscatter diffraction (EBSD)-based crystal orientation mapping, only a single planar section of data can be collected at a time, as sampling is restricted to surfaces. To fully reconstruct 3D microstructures using SEM or EBSD, inherently destructive focused-ion beams

(FIB) or mechanical polishing must be employed to generate serial sections of the sample.<sup>67-70</sup> These techniques cannot be used to directly characterize the dynamics of grain growth. More recently, nondestructive high-energy X-ray diffraction (HEXRD)based orientation mapping has been developed to reconstruct the entire 3D microstructure of bulk materials, 71 even between multiple ex situ processing steps. These experiments have yielded groundbreaking results concerning grain boundary velocities, mobilities and driving forces for migration. 49,72–74 This method is still rapidly developing; at the time of writing, the approach boasts outstanding angular resolution (< 0.1°) with only limited spatial resolution ( $\geq 1 \mu m$ ), requires access to a synchrotron radiation source and employs solely reciprocal space information for microstructural reconstruction.<sup>73</sup> HEXRD of data is still therefore relatively expensive to collect and process and is still relatively coarse in time and space compared to what is now possible in S/TEM instruments present at many institutions.

### STATIC CHARACTERIZATION OF GRAIN GROWTH IN THE TEM

#### **Static Imaging and Characterization**

Due to the relevant microstructural length scale, nanocrystalline thin film materials typically must be characterized using TEM techniques.<sup>75</sup> In their simplest incarnation, conventional TEM approaches leverage diffraction contrast to distinguish grains from one another. The Unfortunately, bright-field TEM images of polycrystalline materials, like those shown in Fig. 1a and b, present certain challenges in their interpretation. In particular, two adjacent grains may have identical diffracted intensities and thus show no contrast, such as the regions labeled "2" in Fig. 1a and b; in addition, the small de Broglie wavelength of the electron beam renders the imaging sensitive to small orientation gradients, resulting in bend contours that are sometimes difficult to distinguish from grain boundaries. Examples of this phenomenon are visible in the regions labeled "1" in Fig. 1a and b. Taking multiple images at a variable beam-sample tilt angle mitigates this issue, as changing the diffraction condition causes contrast between grains to appear and disappear and bend contours to move smoothly across a region.

Conventional gradient-based edge detection algorithms, however, generally fail to accurately segment images into grains and delimiting boundaries or do not readily generalize. <sup>42,66,77</sup> Until recently, the sole method for extracting reliable microstructural information from these types of images was laborious hand tracing of the grain boundary network. <sup>66,78,79</sup> The manual extraction of unbiased and reproducible results from data that are inherently ambiguous requires significant time and expertise. <sup>75</sup> Nonetheless, many data have been collected in this manner, and these data have been

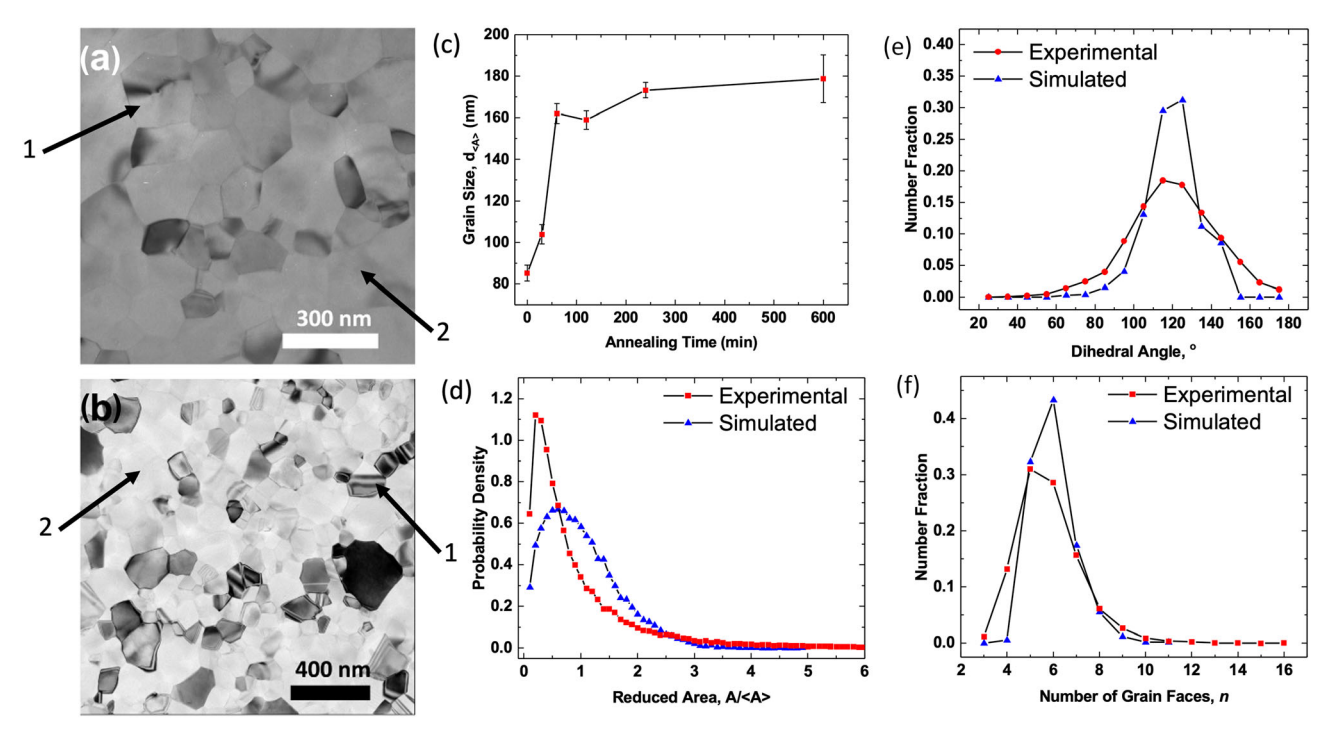


Fig. 1. (a, b) Example BF TEM micrographs of an Al thin film. Regions labeled 1 show bend contours; regions labeled 2 show limited contrast between grains. (c) Typical time profile of grain size for a nominally 100-nm-thick Al thin film annealed at 400°C. (d) Comparison of universal experimental grain size distribution with grain size distributions obtained from a sharp interface model with isotropic boundary energies.<sup>24</sup> (e) Comparison of dihedral angle distributions between experimental results at stagnation and simulated results.<sup>24</sup> (f) Comparison of experimental fraction of grains as a function of grain faces with those for simulations with grain boundary grooving. (a, b) Reproduced from Ref. 66, (c, d) reproduced from Ref. 24, with permission.

extensively compared to, and in many cases shown to disagree with, the results of simulations. <sup>24,26,75,80,81</sup> Without correlations to crystallographic information about the samples, and because of their labor-limited scale, these results have, in fact, generated more questions than they have answered.

In thin films, for example, grain growth stagnates, as seen in Fig. 1c; furthermore, the grain size distribution takes a universal form shown in Fig. 1e, independent of virtually all experimental conditions. This universal distribution has been experimentally observed from hand-traced images of films of various materials at various stages of grain growth.<sup>24,82</sup> The observed stagnation has not yet been fully explained mechanistically. While a simulation of grain growth might match experimental results for a single metric, generally there is disagreement for others, especially those related to topological features such as nearest neighbor correlations. 24,25 In one early case of computer simulations of grain growth, the effects of grooving were modeled, reproducing the experimentally observed stagnation at log-normal distribution of grain sizes;83 yet, as shown in Fig. 1d, front-tracking and sharp interface models still do not capture the distribution of the number of sides of grains in experimental microstructures. 24,26 Even for basic geometric properties, such as dihedral angles at triple junctions, models do not agree with

experimental measurements as illustrated in Fig. 1f. In short, no theory simultaneously explains all experimentally observed aspects of microstructure.

To address these disparities, extensive experiments must be performed to first sample the parameter-space of annealing time and temperature. Unfortunately, tedious manual tracing has long limited the scale of experimental results.7 Some automated methodologies for grain boundary identification in the late 1990 s showed some success, 42 but these approaches did not generalize, and little progress was made in the 2000 s.<sup>77</sup> The software revolutions of the 2010 s, including major advancements in deep learning (DL) and fully convolutional neural networks, have catapulted progress in computer vision, finally opening the door to high-throughput analysis of BF TEM images of nanocrystalline thin films. The most notable architecture in this context is U-Net, first introduced for the segmentation of TEM images of stained biological samples. 84–86 Machine learning approaches for semantic segmentation, including U-Nets, have been applied to solve a wide variety of materials microscopy problems. 65,87,88 In many instances, however, simulated labels have been used as ground truth training data, <sup>89,90</sup> and so the connection with experimental microstructure is, at best, indirect. Unfortunately, due to the complex image formation of conventional TEM images of polycrystals, at the time of writing the only viable source of training data is hand-labeled images; indeed, the quality and quantity of these tracings are important factors in determining the performance of the model.<sup>91</sup>

Recent work has leveraged hand-labeled micrographs as ground truth data to train a model based on the U-Net architecture to solve the longstanding problem of automated grain boundary segmentation in BF TEM micrographs. These approaches identify grain boundaries with minimal artifacts and offer statistically comparable results relative to hand tracings, even for materials unseen during training.66 Given post-processing hyperparameters tuned for a small number of ground-truth labeled images per material, the model generated segmentations comparable to those of expert-generated tracings for Al, Pt and Pd thin films, <sup>66</sup> as shown in Fig. 2, and transfer learning approaches using a small amount of additional training data improve performance on unseen materials. A separate implementation of the architecture employed assumptions about the grain morphology and an implementation of the CHAC algorithm<sup>92</sup> to analyze BF TEM images of nanocrystalline UO2 samples and their microstructural development during in situ irradiation-induced grain growth experiments, without the use of ground truth data for explicit tuning of any post-processing hyperparameters. 79 This work also independently demonstrated that the U-Net model does not require a large amount of training data, generating satisfactory results with about 1000 manually labeled grains in the training set and saturating with 5% improved performance with around 3000 training grains.

Looking ahead, other, unsupervised, techniques might be adopted from those shown to work in optical microscopy applications and other modes. 93,94 Such techniques provide an attractive option to address the artifacts and inherent ambiguity in TEM micrographs. In short, advancements in image processing and computer vision present a path forward for high-throughput analysis of samples processed both ex and in situ at a scale that would not be possible via hand tracing. Nevertheless, no matter the extent of geometric data collected from direct-space images, the description of microstructural evolution is incomplete without accounting for the crystallographic character of the boundaries and the orientation texture of the crystallites.

# Static Orientation Mapping and Grain Boundary Character Distributions

In bulk materials, grain growth is understood to be driven by the reduction in grain boundary energy in the system by the migration of grain boundaries, distinguishing the process from recrystallization where a volumetric driving force is present. 95 Coarsening is primarily accomplished by the net reduction in the total grain boundary area but is also driven by the favored growth of lower energy boundaries relative to their higher energy counterparts. 46,96 Even in samples lacking crystal orientation texture, this growth asymmetry leads to an anisotropic interfacial distribution, known as the grain boundary character distribution (GBCD).<sup>30,31,9</sup>

Representing a given macroscopic boundary character requires five parameters, represented through its misorientation (three parameters) and its plane inclination (two parameters).<sup>98</sup> The misorientation describes the rotation required to bring a given crystal lattice into coincidence with its neighbor across the grain boundary (Fig. 3a and b) and can be represented in one of several equivalent ways,

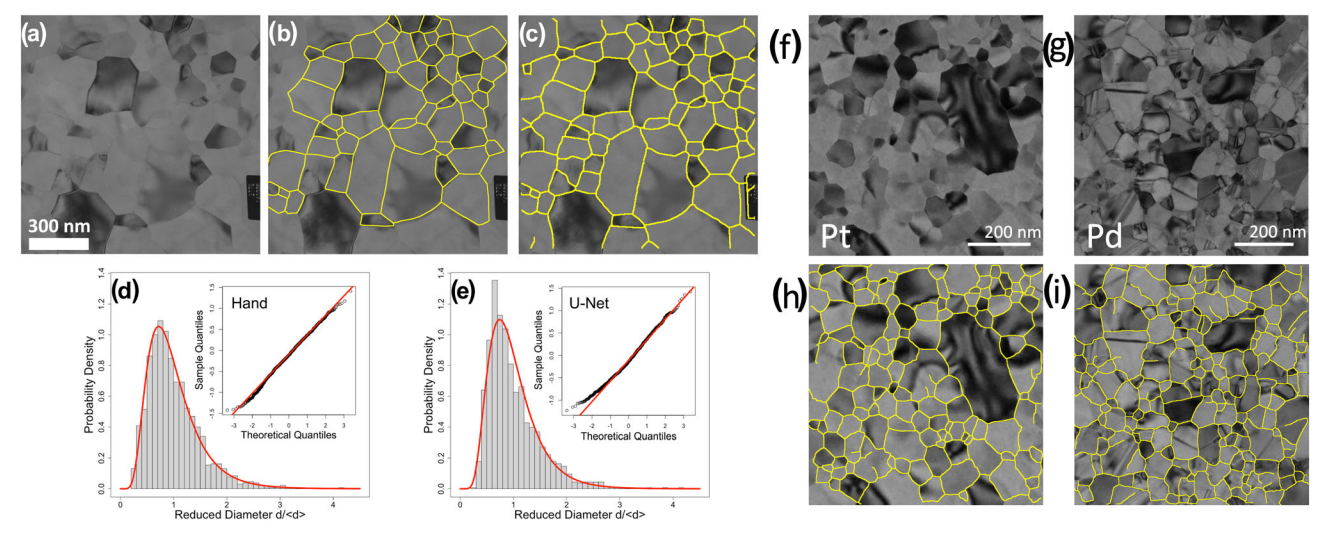


Fig. 2. (a) Bright-field TEM image of a 100-nm Al film with its (b) hand tracing and (c) U-Net + post-processing segmentation overlaid. (d, e) The respective grain size distributions for a set of 1429 manually identified and 1359 automatically identified grains. (f, g) Bright-field TEM images of a 50-nm-thick Pt thin film and 30-nm-thick Pd thin film collected during in situ heating experiments. (h, i) Overlay of the U-Net + post-processing segmentations of these images. Figures reproduced from Ref. 66, with permission.

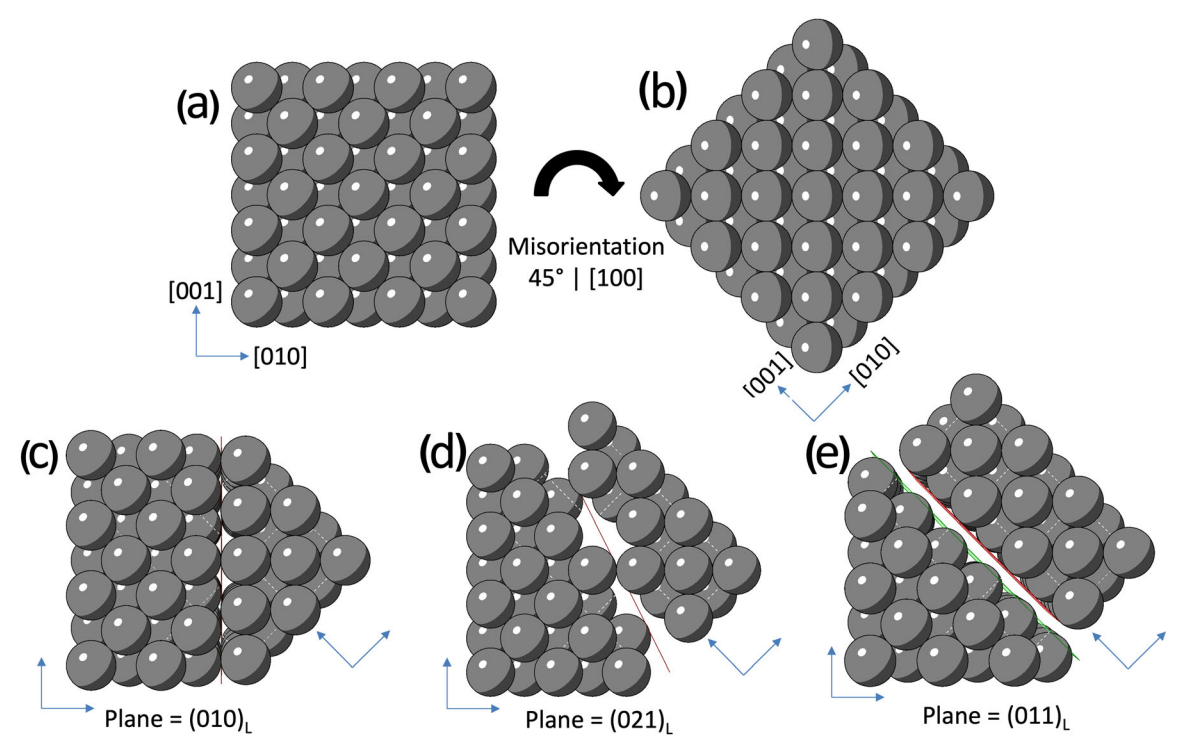


Fig. 3. Schematic representation of (a, b) two fcc crystals with a fixed misorientation of 45° about their shared axis, in this case the [100] direction. (c–e) For this fixed misorientation, three possible grain boundary plane inclinations are shown as examples, having indices (010), (021) and (011) in the reference frame of the left crystal. Note that (c) and (e) are macroscopically equivalent grain boundaries due to crystal-exchange symmetry.

including: by three Euler angles in the Bunge convention, by a rotation matrix or, often most conveniently, as the axis shared between the two crystals and a single disorientation\* angle. The plane inclination is independent of misorientation and describes which crystallographic plane in each crystal divides the two abutting crystals (Fig. 3c, d, and e), as represented in the sample reference frame by its normal vector in spherical coordinates, i.e., two parameters. Figure 3 shows how, for a given misorientation, an arbitrary plane may divide the crystallites.

Given the difficulties associated with grain boundary plane characterization, boundaries are sometimes represented only by their misorientation. This representation is typically couched in terms of a one-parameter misorientation angle, a three-parameter misorientation or a  $\Sigma$ -designation of the coincidence site lattice (CSL) model, but this reduced description is fundamentally incomplete; large anisotropies are observed even for a single misorientation relationship since the grain boundary plane inclination dominates many key properties, such as excess energy. Indeed, the plane inclination plays a key role in determining the nature of the surfaces that participate in the

interface, <sup>99</sup> and the properties of individual boundaries and polycrystalline materials have been documented to be strong functions of the full five-parameter grain boundary character. <sup>100–107</sup> Furthermore, the theoretical treatment of grain boundaries only through the lens of highly symmetric special relationships can lead to incorrect conclusions regarding the behavior of polycrystals. <sup>108</sup>

The distribution of these interfaces in a sample, i.e., the five-parameter GBCD, and related measures are thus indispensable tools for characterizing microstructure and the kinetics of microstructural evolution. Nevertheless, the precise role of GBCD in grain growth is still under investigation. Some recent dynamic experiments, for example, have found that grain boundary character is clearly correlated to dynamic properties like boundary velocity and mobility, and geometric properties like boundary curvature, 49 indicating that the GBCD is central to microstructural development. Other experiments have found no such correlation between the five parameter character of the boundaries and their mobilities, suggesting that atomistic or other physical descriptions are required to fully explain the observed variation in mobilities and velocities. 109

Statically, GBCDs have been measured for a wide variety of bulk materials with grain sizes in the micrometer range using a variety of techniques<sup>47,50,52,53,67,110–113</sup> and have been uniformly observed to be highly anisotropic. Moreover, they

<sup>\*</sup>Due to crystal symmetries, many representations of a single misorientation relationship may be equivalent. The term "disorientation" angle is used here to refer to the representation which requires the smallest angle of rotation among a set of symmetrically equivalent misorientation relationships.

usually show a strong inverse correlation with the material's intrinsic anisotropic grain boundary energy distribution (GBED). 30,114 Measurements of GBCDs were first made using electron backscatter diffraction (EBSD) and serial sectioning, 113 then using stereological analysis of single layers of EBSD or PED data<sup>43,47,115</sup> and more recently using highenergy X-ray diffraction (HEXRD) microscopy. 73,116,117 Serial sectioning and HEXRD microscopy techniques can reconstruct the full 3D microstructure of the material, although only HEXRD is non-destructive and can map the same 3D region of a sample before and after processing steps. In thin films, coarse grained samples with thicknesses on the order of a micrometer can be mapped using EBSD, but the resolution is conventionally limited to 25–100 nm by the Kikuchi pattern source volume. 118 Nanostructured thin films must therefore be investigated using transmission techniques, which include transmission Kikuchi diffraction (TKD) in the SEM (resolution  $\sim 2-$ 10 nm<sup>118</sup>) and TEM-based techniques to reach the spatial resolutions required to resolve the details of the microstructure. In particular, 4D-STEM techniques like scanning precession enhanced electron diffraction (PED)-based mapping have brought the spatial resolution of orientation maps down to 1 nm, although this advance comes with a tradeoff of lower orientation angular resolutions of only 0.5°-1°, since indexing is based on spot patterns rather than Kikuchi lines.<sup>58</sup> Importantly, for most hard materials, these are nondestructive techniques that in principle allow for the analysis of the same region between processing steps.

PED mapping has been used to characterize the microstructures and GBCDs of thin films of copper, aluminum and tungsten. 47,52,115,119,120 The results have conclusively demonstrated that, absent strong orientation texture, the GBCDs of materials are largely invariant to grain size and sample geometry, except for elevated populations of coherent twins in films. 47,50 Figure 4b, d, and f shows this correlation between several thin film materials and comparable bulk materials. Since grain boundary energies would not be expected to vary as a function of sample and grain geometry, 30,114 it is perhaps unsurprising that films lacking orientation texture retain the GBCD texture observed in bulk materials. Indeed, in both the bulk and nanocrystalline thin film cases, the populations of grain boundaries show a distinct log-linear inverse correlation with their computed energies. Figure 4a, c, and e illustrates this inverse correlation for several materials, including bulk and thin film samples, where it is evident that the lowest energy boundaries occur with the greatest frequency compared to a random distribution, and the highest energy boundaries occur with the lowest frequency when similarly normalized.

#### Thin Film Considerations for Grain Boundary Character Distribution

While evidence suggests that in bulk materials the GBCD develops by preferential elimination of higher energy grain boundaries during grain growth, 97,121–123 in thin films the common GBCD has been observed in as-deposited films of Al, Cu and in films of W which did not experience any significant post-deposition grain growth. 47,52,53 These GBCDs still exhibit an inverse correlation with their expected GBEDs, 124-128 indicating that grain boundary selection is an important energy reducing factor in the very earliest stages of film formation. Indeed, the GBCD of Al and Cu films, when compared to bulk samples of the same materials, show a significantly larger population of the very low energy coherent twin boundaries, which likely form as the film coalesces. 47,53 It is argued that large atomic mobilities result in relatively unconstrained crystallite orientations during film formation. 129,130 This permits the nonrandom selection of interfaces between neighboring crystallites, favoring lower energy grain boundaries.<sup>47</sup> In thin films, however, the large relative contribution of the top and bottom surfaces to the system's total energy favors grain orientations with high atomic packing at the external interfaces. <sup>2,131–134</sup> This results in grains with lower surface energies [e.g., grains oriented with the (111) plane parallel to the plane of the film in fcc materials] growing at the expense of grains terminating at free surfaces of greater interfacial energies and driving the development of orientation texture. 1,2,135

As this orientation texture develops in thin films, geometric constraints dictate the available grain boundary planes for a given misorientation. Consider the case of a columnar thin film, like that represented in the inverse pole figure maps in Fig. 4. As annealing proceeds, the sample develops a stronger (111)-fiber texture. Here, a large fraction of grains is oriented with the (111) plane parallel to the surface of the film with concomitant free inplane orientations. In this case, any two (111)oriented grains are constrained to have a common [111] axis of misorientation, and because no two {111}-type planes are perpendicular to one another, a  $\Sigma 3$  boundary (60° | [111]) between these grains cannot be a coherent twin and instead must be a [111]-tilt boundary. For this misorientation, these are relatively high-energy boundaries, yet their formation is favored during grain growth. This behavior can be seen in Fig. 4d, e, and f where the average  $\Sigma 3$  grain boundary has an ever greater preference for higher energy boundaries as the sample is annealed and develops a stronger orientation texture.

The unique geometric constraints associated with thin films suggest other theoretical questions for the study of microstructural evolution in these polycrystalline systems. Take for example the extraction

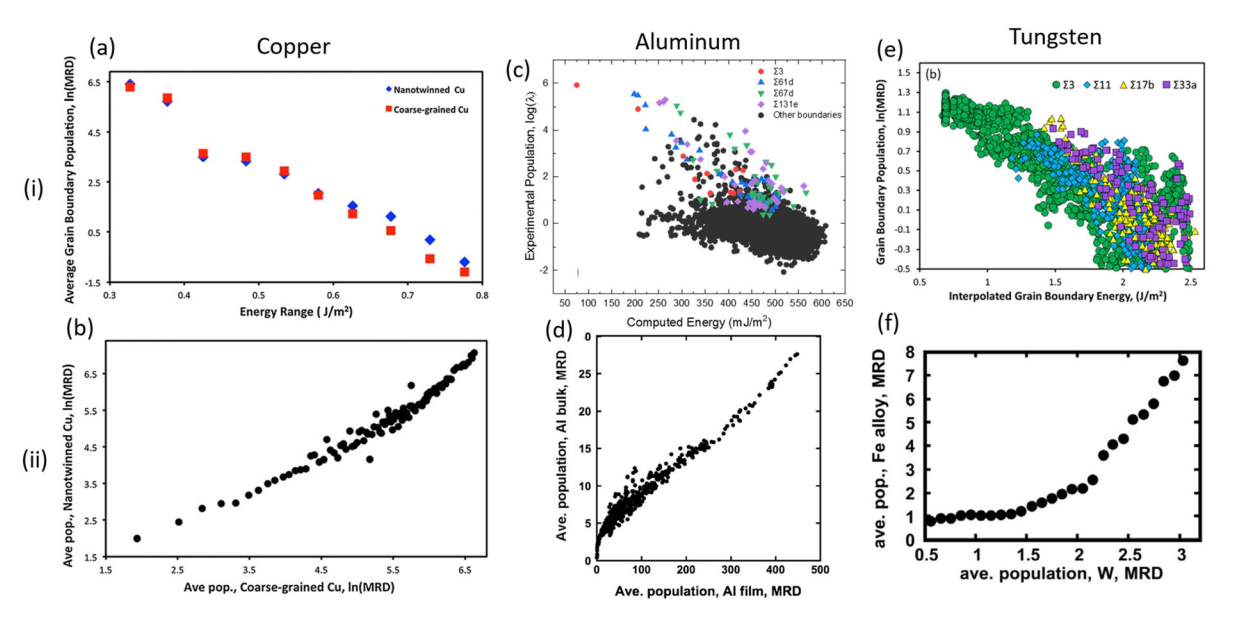


Fig. 4. (i) Experimental populations of grain boundaries in thin film samples, binned by the population as a multiple of the random distribution and by their energies, determined experimentally for (a) Cu, and computed by molecular dynamics for (c) Al and (e) W. (ii) Experimental populations of grain boundaries in nanocrystalline films compared to comparable bulk materials for (b) Cu, (d) Al and (f) W. (a, b) Reproduced from Ref. 50, (c, d) reproduced from Ref. 124, (e) reproduced from Ref. 114 and (f) reproduced from Ref. 52 with permission.

of relative energies from triple junction geometries. To retain stable configurations, grain boundaries must meet at triple junctions; the geometry at these junctions, i.e., the dihedral angles formed between the boundaries and the inclination of the triple line, is governed by a force balance between the normal and tangential forces on the boundaries related to the anisotropy of grain boundary energy; this relationship is embodied the Herring equation.<sup>3</sup> In bulk materials, the capillarity vector formulation of this particular equation 136-139 has been repeatedly used to extract relative grain boundary energies from triple junction geometries 140,141 from 3D reconstructions of the microstructures in a variety of metallic and ceramic systems  $^{30,67,112,142,143}$  This approach has been validated via comparisons with molecular dynamics (MD) calculations of grain boundary energies as well as universal reproducibility of the log-linear inverse correlation between grain boundary energies and populations. 30,47,50,124,125,143-147

Because of the columnar microstructure of thin films, triple junction lines in these systems are almost uniformly perpendicular to the surfaces of the film, and thus an approximate reconstruction of the 3D microstructure is possible from just one layer of PED data. In this situation, similar relative energy reconstruction techniques can, in principle, be applied to these microstructures as well. However, for both films that have experienced grain growth and those that have not, it has been found that the Herring equation does not fully describe the energetics of the system. In particular, it was demonstrated that for a series of Al and W thin films

the relative grain boundary energies extracted from triple junction geometry using the method introduced by Shen et al. He were neither correlated to energies calculated via MD nor inversely correlated to boundary populations, with the notable exception of boundaries with the greatest energetic anisotropy in aluminum (including the  $\Sigma 3$  and  $\Sigma 5$  boundaries, with misorientations about the [111] axis). He was also should be sufficiently suffi

As shown in Fig. 5, however, in nanocrystalline thin films, the measured grain populations do show an inverse correlation with grain boundary energy as calculated via MD, absent strong orientation texture. This finding indicates that while the thermodynamics of grain boundary character selection remain largely unchanged, factors not considered in the conventional Herring analysis control the behavior of the grain boundaries near triple junctions and represent forces on the boundaries which compete with those included in the Herring equation. As noted above, in cases where the energy anisotropy of the grain boundaries is large, the Herring equation does describe the system, indicating that, in these situations, the grain boundary energy anisotropy dominates the triple junction geometry. Indeed, for the case of coherent twins as an example, the dominance of the driving force toward (111) inclinations of planes for  $\Sigma 3$  misorientations leads, in many cases, to boundaries inclined relative to the columnar approximation. For other boundaries, particularly those with misorientation axes outside of the < 111> family, other documented drivers of boundary migration and grain growth, including the geometric driving force toward columnarity, free-surface energy and

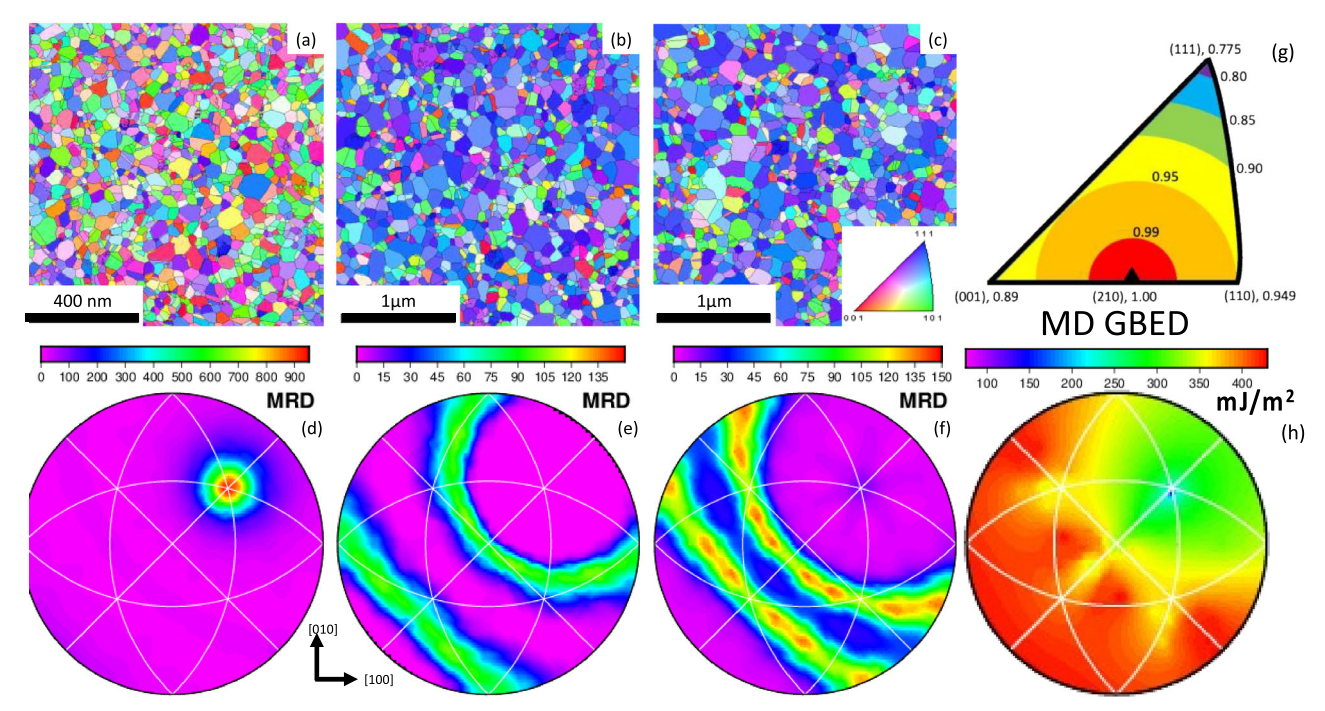


Fig. 5. Inverse pole figure maps for a 100-nm-thick AI thin film (a) as-deposited, (b) after 30 min at 400°C and (c) after 150 min at 400°C. The orientation texture increases from 2.6 MRD to 6.0 MRD preference for the [111]. (d–f) Corresponding grain boundary plane distributions for the  $\Sigma$ 3 misorientation. (g) Relative surface energies for crystal orientations in fcc materials, following the broken bond model<sup>131,132</sup> (h) Grain boundary energy distribution the  $\Sigma$ 3 misorientation as a function of grain boundary plane for AI as computed by molecular dynamics.<sup>124,128</sup> (a–f, h) reproduced from Ref. 124, with permission.

strain energy,<sup>133</sup> likely have a greater relative magnitude compared with the energy associate with capillarity forces and thus exert notable influence on the triple junction geometry. Ultimately, these considerations render the conventional Herring equation an incomplete descriptor of thin film systems and indicates that the geometric constraints of the films do play a non-negligeable role in the grain boundary network behavior.

Despite the expanded understanding of thin film microstructural behavior offered by orientation mapping, these techniques suffer from a key drawback, namely significant acquisition time, and therefore cannot be used to characterize evolving systems. Recent developments in direct electron detector technologies and 4D-STEM techniques have pushed the frontiers of PED-based orientation mapping and have the potential to further increase spatial resolution and rate of acquisition for thin film materials. Nevertheless, cost, data storage and acquisition rate constraints remain problematic for the requisite enormous data collection.

# DYNAMIC CHARACTERIZATION OF GRAIN GROWTH IN THE TEM

# **Information Technology and Instrumentation for In Situ TEM Experiments**

In situ study of grain growth in the TEM has been of interest for decades, <sup>149</sup> but early heating experiments suffered from the large thermal mass of

holders, samples and stages that contributed to long temperature ramp times, inconsistent temperatures and substantial thermal drift. All told, these limitations rendered studies of the dynamics of grain growth impractical. Furthermore, as noted above, automated approaches for reproducibly identifying grain boundaries in a large number of TEM micrographs, especially those leveraging artificial intelligence techniques developed in the past decade, 79,86 have only just been introduced.

The advent of microelectromechanical systems (MEMS), including heating chips with precise temperature control and low thermal mass, as well as chips that can strain samples, apply electrical biases or control liquid and gas environments, has enabled a revolution in in situ studies of a wide variety of phenomena, from catalysis to nucleation and growth. 150 For heating experiments, chips with electron transparent windows with or without support films have been developed with the ability to quickly ramp up temperatures. Although only a small region of the chip is heated, the thermal drift is still of concern for high-resolution imaging. This drift effect has become more manageable, even over only the past few years, 64 thanks to commercially available machine-vision driven drift correction and data management solutions like AXONTM from Protochips (Morrisville, NC). Today, the confluence of technologies required to perform large-scale in situ studies of grain growth in the TEM positions the thin film grain growth community at the

precipice of a revolution in experimental capabilities. In the following sections, we summarize the ways in which these innovations can be leveraged for studies in the very near future and discuss novel frameworks to understand the analysis of these large, complex and dynamic datasets.

# **Dynamic Grain Growth Experiments** in the TEM: Imaging

Using modern hardware and software solutions, it has recently become possible to capture a series of drift corrected images during in situ annealing of nanocrystalline thin films deposited on specialized MEMS chips. Paired with modern charge coupled device (CCD) cameras, frame rates of around 1 fps can be captured. Using more recent direct electron detector (DED) technology, <sup>151</sup> these rates may be further increased. In the foreseeable future, however, the cost of these detectors may outweigh the benefits for studies of grain growth, which typically are performed on time scales of minutes to hours. Indeed, these experiments are generally still in their early stages. Thus far, in situ TEM studies of grain growth in nanocrystalline thin films have been used to analyze the process of grain growth at the population level and grain boundary migration at the level of individual boundaries and grains, with impressive, if not yet transformative, results. Studies have yet to treat the problem holistically, integrating local boundary migration information with broader information collected on the entire network, partly because experimental capabilities are still being actively developed and partly because the frameworks for analyzing this type of crosscutting microstructural data are still in their infancy.

As one example of such experiments, a nanocrystalline copper film annealed in situ in the TEM, the growth kinetics, average grain boundary velocities and average mobilities were estimated, experimentally confirming that the driving force for boundary migration is much higher in nanocrystalline Cu than in its microcrystalline counterpart. An increased density of coherent twins was also observed by local analysis, consistent with ex situ PED orientation mapping-based experiments on copper samples with large grain population statistics. 119 In another study, concerning an ultrafinegrained titanium film, the effect of the thickness of the film on grain growth and recrystallization behavior was investigated via in situ TEM imaging. 153 It was demonstrated that in a foil of variable thickness, the growth rate and stagnant size of grains after annealing correlated with the film thickness. Again, statistics regarding the aggregate material are reported in the different regions, but only a select number of grains and grain boundaries is tracked individually, and little is uncovered concerning the kinetics of grain growth and boundary migration in the different thickness regimes. In

this work, grain growth stagnation is attributed to grain boundary grooving, observed via atomic force microscopy across select boundaries, but no statistically significant population of grains is investigated, and the nature of the grooving is not analyzed in detail.

Grain growth can also be induced via stress in the material, as has been observed in situ in thin films. $^{154-156}$  In an Al thin film study, $^{155}$  for example, it was clearly demonstrated that in regions experiencing significant plastic deformation and necking, grains experienced much greater coarsening relative to regions which experienced lower true stresses and less plastic deformation. Large-scale local measurements of grain boundaries and grains were not performed; instead, the evolution of selected grains and associated boundaries was directly characterized, and the global microstructural evolution is captured using PED measurements before and after deformation. Unfortunately, the rich crystallographic information available from the orientation mapping is not integrated into the analysis of the grain coarsening. In a similar study of coarsening in a 75-nm Pt film, <sup>154</sup> interesting conclusions are drawn about the driving forces for boundary migration near a crack tip, but because no crystallographic information about the grains is available, and the vast space of boundary parameters is not sampled, little is revealed for the general case of grain growth.

In other cases, individual boundaries or grains are studied in great detail. For example, conventional and high-resolution TEM and scanning TEM (S/TEM) have been used to study the migration of boundaries at the atomic scale under the irradiation of the electron beam, <sup>157,158</sup> as a result of thermal annealing <sup>159</sup> or under mechanical stress <sup>160</sup> to better understand the underlying mechanisms of grain boundary migration. In situ observations of crystal growth in amorphous matrices do not suffer from many of the limitations that have been encountered for grain growth measurements, and so these experiments at statistically meaningful scale have been possible for decades. 161,162 Still, recent observations have been made using STEM imaging of the appearance and growth of individual grains, for example, in Zr-doped In<sub>2</sub>O<sub>3</sub> films during an amorphous to crystalline transition. Recent advances in Bragg coherent X-ray diffraction imaging further enabled the full characterization of the 3D structure of individual grains in impressive detail.<sup>163</sup> The results of this work showed single grain growth in the amorphous matrix is interface controlled, leading to growth anisotropy in the film. Despite the greater detail available, however, this treatment still only examines a small number of grains and the data presented here are not suited to address the more general grain growth scenario.

While the goals of the existing in situ studies are varied and not necessarily oriented toward developing generalized explanations for grain growth, their common limitation is one of scale for both data collection and analytics. Identification of grains and grain boundaries in a high-throughput and automated fashion, appropriate for large-scale in situ data acquisition, vastly improves the available grain population by overcoming the bottleneck inherent to the generation manual tracings. These automated techniques have already been useful for in situ characterization of grain growth, 78,164 but studies which examine population-level behavior of the grain size using such automated approaches are only beginning to appear. 79 Nevertheless, determining which grains grow or shrink and how this behavior is determined by their geometric, topological and crystallographic characteristics remains a priority for understanding grain growth. While much work remains in optimizing and conducting experiments, as well as developing data mining techniques to extract quantitative information from automated segmentations, the tools which now exist and those which are currently in development position thin films as a prime platform for the next generation ofimage-based grain experiments.

# Frontiers: Correlative Electron Microscopy for Grain Growth Studies

Direct BF TEM imaging of grain growth is unrivaled in spatial-temporal resolution and is the only technique available to directly resolve the complete geometric evolution of a microstructure in real-time. Unfortunately, these images do not contain any detailed information about the crystallographic orientation and therefore lack any information about the crystallographic character of the grain boundaries. This is a critical omission. While orientation mapping is too slow to be used to acquire data in real time during microstructural evolution, valuable insights can still be obtained during heating experiments by intermittently measuring grain orientations. This can be accomplished straightforwardly in the TEM since the instrumentation required to perform direct-space imaging is identical with that required for orientation mapping. Thus, the same region imaged during evolution can be seamlessly characterized using S/TEM-based orientation mapping, keeping the same sample region in the imaging path of the electron beam.

Figure 6 shows an example of this type of experiment for a 30-nm-thick Pd film, with bright-field TEM images captured near the beginning and near the end of a heating step at 400°C shown alongside PED orientation maps acquired before and after the heating step. This type of experiment is still preliminary, but similar frameworks have already begun appearing in archival conference papers and have led to initial characterizations of grain growth in thin films. As an example, a recent study provides evidence of a correlation between grain rotation and grain growth during in situ

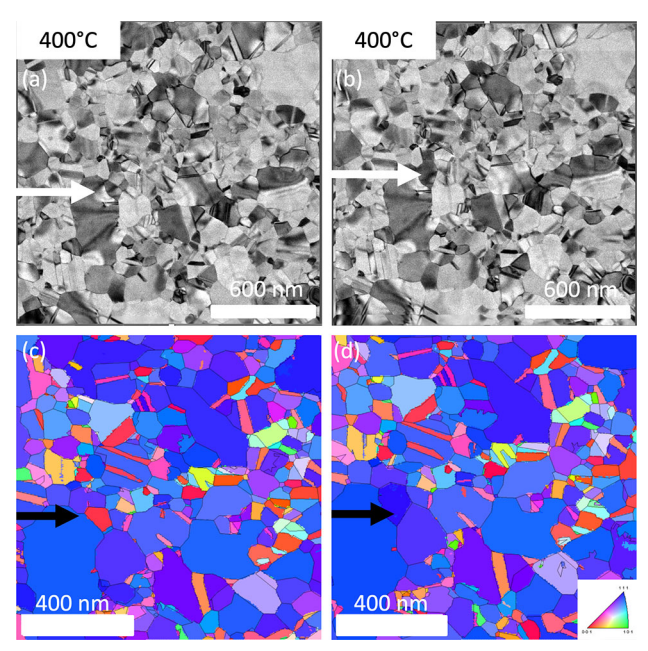


Fig. 6. Bright-field images of a 30-nm-thick Pd film sputter deposited onto a MEMS heating chip captured during an in situ heating experiment (a) before and (b) after 45 min at 400°C, with inverse pole figure maps shown of the same region (c) before and (d) after annealing. Arrows indicate a region which experienced evolution.

heating experiments in nanocrystalline Pt films. <sup>165</sup> Another study, concerning a nanocrystalline nickel sample, discovered reversible lattice rotations during deformation using dark-field image-based 3D orientation mapping in the TEM. <sup>60</sup> Despite their promise, however, the value of integrated image-and orientation-based measurements remains to be proven for grain growth studies. Reliable feature tracking in time, for example, remains a significant problem for this type of experiment.

# Data Analytics and Model Integration of Dynamic Grain Growth Experiments

Given the aforementioned advances in experimental interrogation of grain growth and associated data collection in thin films, it is now becoming possible to draw statistically meaningful conclusions from quantitative analyses of sufficiently large datasets. These analyses typically focus on correlations existing among key microstructural features and the information content of discretized images. In conjunction with such studies, various mathematical descriptions of grain coarsening (e.g., multistate spin models, 166,167 phase-field models and triple-junction motion models 34,36) have been advanced that capture much of the underlying physics of coarsening in these and related systems. We note, however, that these models typically require inputs of energetic and dynamic information (i.e., grain-boundary excess energies, mobilities and related parameters) that must be obtained from experiments and/or computer simulations of atomic-

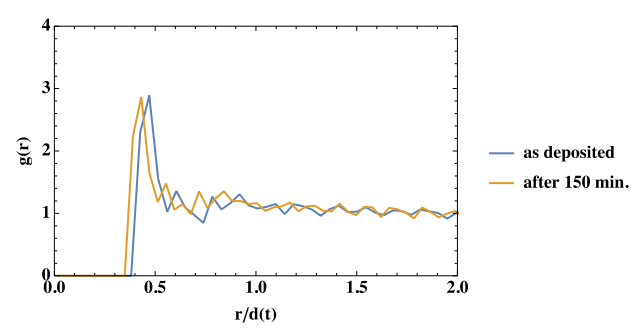


Fig. 7. The radial distribution function, g(r) versus scaled distance where r is the triple-junction separation and d(t) is the (time-dependent) effective circular grain diameter, for an as-deposited Al film (blue line) and for one annealed for 150 min (gold line) at a temperature T = 400°C. (Reprinted from Ref. 170 under the CC-BY license) (Color figure online).

scale behavior. Thus, one current challenge in the formulation of physically realistic models of coarsening is the establishment of a direct connection between these models and grain growth experiments.

Several descriptors of coarsening can be obtained from TEM micrographs of evolving polycrystalline thin films. For this purpose, it is convenient to focus on markers that may be identified and tracked experimentally in a micrograph. For example, one can regard the collection of triple junctions in a given microstructure as a representative configuration of a marked (non-Poisson\*\*) point process, with the marks representing the three grain disorientations associated with each junction. <sup>169</sup>

With this framework, triple junctions interact to a good approximation via pair potentials specific to the grain disorientations associated with a given junction. These potentials may be determined from calculations of the associated static, triple-junction (partial) correlation functions and embody grain-boundary energetics. More specifically, the triple-junction radial distribution function, g(r), summarizes the conditional probability of finding a triple junction at a distance r from a given triple junction. Figure 7 shows the calculated value of the radial distribution function from an analysis of PED orientation maps of 100 nm-thick, sputter-deposited Al films.  $^{170}$ 

It is also useful to quantify the complexity of a microstructure as a proxy for the microstructural entropy. We note first that the pair correlation function described above may be employed for this purpose; <sup>170</sup> other authors have suggested a Shannon entropy based on the grain-size distribution. <sup>171</sup> More recently, Rickman et al. <sup>172</sup> advanced two complementary microstructural complexity measures based on (1) compressed strings that embody the information contained in the time evolution of a system and (2) the spectra of graph Laplacians that reflect the information contained in a coarsening

microstructure. These approaches permit the characterization of dynamically evolving microstructures and the identification of associated correlation times, providing a bridge to existing theoretical frameworks for analyzing grain growth.

#### CONCLUSION AND OUTLOOK

Grain growth behavior is essential to understanding the processing-structure and structure-performance characteristics of polycrystalline materials, yet no prescriptive theory exists which allows scientists and engineers to map a path from a starting microstructure to a final structure. Still, studies of grain growth have seen major developments in recent years, especially with the advent of automated orientation mapping techniques like automated FIB serial sectioning and EBSD and HEXRD for bulk microcrystalline materials and PED-based 4D-STEM for nanocrystalline thin film materials. The five-parameter grain boundary character distribution has emerged from these measurements and has been established as a critically important factor in describing microstructure, emphasizing the importance of both the full character of the grain boundary network on properties and structural evolution as well as the analogous behavior of bulk and thin film materials.

Due to their simplified 3D structure, thin films offer a robust experimental platform for studying grain growth. Columnar grains and one-stop, nondestructive characterization render thin films ideal candidates for seamless TEM-based in situ correlative microscopy, weaving direct-space imaging together with crystal orientation data with spatial and temporal resolution in a way which is not currently possible in bulk materials. Technological advances in MEMS chip technology, computer-vision driven drift correction, deep learning-based image segmentation and increases in computational power and digital storage capacity have brought this type of experiment to the frontier of possibility, offering a unique opportunity for the large-scale data acquisition and mining required to integrate the myriad of observations and microstructural metrics into theoretical and mathematical frameworks in service of a more complete and prescriptive theory of grain growth.

#### **ACKNOWLEDGMENTS**

The authors gratefully acknowledge financial support from the United States National Science Foundation under grant DMS-1905492 and under the DMREF program grants DMS-2118206 and DMS-2118197. This work was carried out in part in the Electron Microscopy Laboratory of Columbia Nano Initiative (CNI) Shared Lab Facilities at Columbia University.

<sup>\*\*</sup>This point process is non-Poissonian owing to effective interactions between the triple junctions.

#### CONFLICT OF INTEREST

On behalf of all authors, the corresponding author states that there is no conflict of interest.

#### REFERENCES

- 1. C.V. Thompson, Annu. Rev. Mater. Sci. 20, 245 (1990).
- 2. C.V. Thompson, Annu. Rev. Mater. Sci. 30, 159 (2000).
- B.E.K.Z.C. Cordero, and C.A. Schuh, *Int. Mater. Rev.* 61, 495 (2016).
- 4. L.C. Lim, and T. Watanabe, Scr. Metall. 23, 489 (1989).
- 5. N.J. Petch, J. Iron Steel Inst. 174, 25 (1953).
- 6. E. Hall, Proc. Phys. Soc. Sect. B 64, 747 (1951).
- E.M. Lehockey, G. Palumbo, A. Brennenstuhl, and P. Lin, Mater. Res. Soc. Symp. – Proc. 458, 243 (1997).
- T. Liu, S. Xia, Q. Bai, B. Zhou, L. Zhang, Y. Lu, and T. Shoji, *Materials* 12, 242 (2017).
- 9. E.M. Lehockey, G. Palumbo, P. Lin, and A.M. Brennenstuhl, Scr. Mater. 36, 1211 (1997).
- 10. Y. Mishin, and C. Herzig, Mater. Sci. Eng. 260, 55 (1999).
- E.A. Jägle, and E.J. Mittemeijer, Acta Mater. 59, 5775 (2011).
- K. Barmak, X. Liu, A. Darbal, N. T. Nuhfer, D. Choi, T. Sun, A. P. Warren, K. R. Coffey, and M. F. Toney, *J. Appl. Phys.* **120** (2016).
- K. Barmak, A. Darbal, K.J. Ganesh, P.J. Ferreira, J.M. Rickman, T. Sun, B. Yao, A.P. Warren, and K.R. Coffey, J. Vac. Sci. Technol. A 32, 61503 (2014).
- T. Sun, B. Yao, A. P. Warren, K. Barmak, M. F. Toney, R. E. Peale, and K. R. Coffey, *Phys. Rev. B Condens. Matter Mater. Phys.* 81 (2010).
- 15. W.W. Mullins, Acta Metall. 6, 414 (1958).
- G. Gottstein, and L.S. Shvindlerman, Scr. Mater. 38, 1541 (1998).
- 17. D. Zöllner, and P.R. Rios, Acta Mater. 70, 290 (2014).
- J. Hu, X. Wang, J. Zhang, J. Luo, Z. Zhang, and Z. Shen, J. Materiomics 7, 1007 (2021).
- J. Hu, J. Zhang, X. Wang, J. Luo, Z. Zhang, and Z. Shen, J. Materiomics 7, 1014 (2021).
- L. Zhang, J. Han, D. J. Srolovitz, and Y. Xiang, Npj Comput. Mater. 7, 1 (2021).
- 21. E.A. Holm, and S.M. Foiles, Science 328, 1138 (2010).
- 22. M. Hillert, Acta Metall. 13, 227 (1965).
- 23. W. Mullins, J. Appl. Phys. 27, 900 (1956).
- K. Barmak, E. Eggeling, D. Kinderlehrer, R. Sharp, S. Ta'Asan, A. D. Rollett, and K. R. Coffey, *Prog. Mater. Sci.* 58, 987 (2013).
- P.R. Rios, and D. Zöllner, *Mater. Sci. Technol. (UK)* 34, 629 (2018).
- G. Martine La Boissonière, R. Choksi, K. Barmak, and S. Esedolu, Materialia (Oxford) 6, 100280 (2019).
- V.E. Fradkov, A.S. Kravchenko, and L.S. Shvindlerman, Scr. Metall. 19, 1291 (1985).
- G.B. Bizana, and L.A. Barrales-Mora, Comput. Mater. Sci. 219, 112009 (2023).
- C.S. Kim, A.D. Rollett, and G.S. Rohrer, Scr. Mater. 54, 1005 (2006).
- 30. G.S. Rohrer, J. Mater. Sci. 46, 5881 (2011).
- 31. G.S. Rohrer, Ann Rev Mater Res 35, 99 (2005).
- G. Gottstein, and L.S. Shvindlerman, Acta Mater. 50, 703 (2002).
- 33. J.W. Cahn, Acta Metall. 10, 789 (1962).
- Y. Epshteyn, C. Liu, and M. Mizuno, SIAM J. Math. Anal. 53, 3072 (2021).
- D. Mattissen, D.A. Molodov, L.S. Shvindlerman, and G. Gottstein, Acta Mater. 53, 2049 (2005).
- Y. Epshteyn, C. Liu, and M. Mizuno, Commun. Math. Sci. 19, 1403 (2021).
- 37. W.W. Mullins, J. Appl. Phys. 28, 333 (1957).
- C. Herring, and W. Kingston, The Physics of Powder Metallurgy (McGraw Hill, New York, 1951).
- 39. M. Frary, and C.A. Schuh, Acta Mater. 51, 3731 (2003).

- C.A. Schuh, M. Kumar, and W.E. King, J. Mater. Sci. 40, 847 (2005).
- B. W. Reed and C. A. Schuh, in *Electron Backscatter Diffraction in Materials Science*, edited by A. J. Schwartz, M. Kumar, B. L. Adams, and D. P. Field, 2nd ed. (Springer US, New York, 2009), pp. 201–214.
- D.T. Carpenter, J.M. Rickman, and K. Barmak, J. Appl. Phys. 84, 5843 (1998).
- D. M. Saylor, B. S. El-Dasher, B. L. Adams, and G. S. Rohrer, Metall. Mater. Trans. A Phys. Metall. Mater. Sci. 35A, 1981 (2004).
- G. S. Rohrer, D. M. Saylor, B. El Dasher, B. L. Adams, A. D. Rollett, and P. Wynblatt, Zeitschrift Fuer Metallkunde/ Mater. Res. Adv. Tech. (2004).
- Y.-F. Shen, S. Maddali, D. Menasche, A. Bhattacharya, G.S. Rohrer, and R.M. Suter, *Phys Rev Mater* 3, 63611 (2019).
- Z. Xu, C.M. Hefferan, S.F. Li, J. Lind, R.M. Suter, F. Abdeljawad, and G.S. Rohrer, Scr. Mater. 230, 115405 (2023).
- G.S. Rohrer, X. Liu, J. Liu, A. Darbal, M.N. Kelly, X. Chen, M.A. Berkson, N.T. Nuhfer, K.R. Coffey, and K. Barmak, J. Mater. Sci. 52, 9819 (2017).
- 48. K. N. Zhu, Q. Ruan, and A. Godfrey, IOP Conf. Ser.: Mater. Sci. Eng. (2015).
- A. Bhattacharya, Y. F. Shen, C. M. Hefferan, S. F. Li, J. Lind, R. M. Suter, C. E. Krill, and G. S. Rohrer, *Science* (1979) 374, 189 (2021).
- S. Ratanaphan, D. Raabe, R. Sarochawikasit, D.L. Olmsted, G.S. Rohrer, and K.N. Tu, J. Mater. Sci. 52, 4070 (2016).
- V. Randle, G. S. Rohrer, H. M. Miller, M. Coleman, and G. T. Owen, Acta Mater. 56, (2008).
- X. Liu, D. Choi, H. Beladi, N.T. Nuhfer, G.S. Rohrer, and K. Barmak, Scr. Mater. 69, 413 (2013).
- A. Darbal, K. Ganesh, K. Barmak, G. Rohrer, P. Ferreira,
   T. Sun, and K. Coffey, Microsc. Microanal. 17 (2011).
- J. Kang, K. Walter, H. Bale, and A.J. Shahani, *Acta Mater*. 240, 118316 (2022).
- E. F. Rauch, P. Harrison, X. Zhou, M. Herbig, W. Ludwig, and M. Véron, Symmetry, 13, 1675 (2021).
- E.F. Rauch, J. Portillo, S. Nicolopoulos, D. Bultreys, S. Rouvimov, and P. Moeck, Zeitschrift Fur Kristallographie 225, 103 (2010).
- E.F. Rauch, and L. Dupuy, Arch. Metall. Mater. 50, 87 (2005).
- 58. K. Barmak, in Metallic Films for Electronic, Optical, and Magnetic Applications, edited by K. Barmak and K. Coffey
- (Woodhead Publsihing, Philadelphia, 2014), pp. 121–233.
  59. E.F. Rauch, and M. Véron, *Microsc. Microanal*. 22, 500 (2016).
- Q. He, S. Schmidt, W. Zhu, G. Wu, T. Huang, L. Zhang, D.J. Jensen, Z. Feng, A. Godfrey, and X. Huang, Science 382, 1065 (2023).
- H. H. Liu, S. Schmidt, H. F. Poulsen, A. Godfrey, Z. Q. Liu, J. A. Sharon, and X. Huang, *Science* (1979) 332, 833 (2011).
- G. Wu, W. Zhu, Q. He, Z. Feng, T. Huang, L. Zhang, S. Schmidt, A. Godfrey, and X. Huang, Nano Mater. Sci. 2, 50 (2020).
- W. Zhu, G. Wu, A. Godfrey, S. Schmidt, Q. He, Z. Feng, T. Huang, L. Zhang, and X. Huang, Scr. Mater. 214 (2022).
- M.L. Taheri, E.A. Stach, I. Arslan, P.A. Crozier, B.C. Kabius, T. LaGrange, A.M. Minor, S. Takeda, M. Tanase, J.B. Wagner, and R. Sharma, *Ultramicroscopy* 170, 86 (2016).
- E.A. Holm, R. Cohn, N. Gao, A.R. Kitahara, T.P. Matson,
   B. Lei, and S.R. Yarasi, Metall. Mater. Trans. A Phys. Metall. Mater. Sci. 51, 5985 (2020).
- M.J. Patrick, J.K. Eckstein, J.R. Lopez, S. Toderas, S.A. Asher, S.I. Whang, S. Levine, J.M. Rickman, and K. Barmak, *Microsc. Microanal.* 29, 1968–1979 (2023).
- S.J. Dillon, and G.S. Rohrer, J. Am. Ceram. Soc. 92, 1580 (2009).
- M.D. Uchic, M.A. Groeber, D.M. Dimiduk, and J.P. Simmons, Scr. Mater. 55, 23 (2006).

- S. J. Dillon and G. S. Rohrer, Microsc. Microanal. 15(Suppl 2), (2009).
- P.G. Kotula, G.S. Rohrer, and M.P. Marsh, MRS Bull. 39, 361 (2014).
- G. Johnson, A. King, M.G. Honnicke, J. Marrow, and W. Ludwig, J. Appl. Crystallogr. 41, 310 (2008).
- V. Muralikrishnan, H. Liu, L. Yang, B. Conry, C.J. Marvel, M.P. Harmer, G.S. Rohrer, M.R. Tonks, R.M. Suter, C.E. Krill, and A.R. Krause, Scr. Mater. 222, 115055 (2023).
- J.V. Bernier, R.M. Suter, A.D. Rollett, and J.D. Almer, *Annu. Rev. Mater. Res.* 50, 395 (2020).
- A. Bhattacharya, Y.F. Shen, C.M. Hefferan, S.F. Li, J. Lind, R.M. Suter, and G.S. Rohrer, *Acta Mater.* 167, 40 (2019).
- D.T. Carpenter, J.R. Codner, K. Barmak, and J.M. Rickman, *Mater. Lett.* 41, 296 (1999).
- D.B. Williams, and C.B. Carter, Transmission electron microscopy: a textbook for materials science (Springer, USA, 2009).
- J. S. Chambers, Masters Thesis, Duquesne University (2006).
- M. J. Patrick, J. K. Eckstein, J. Lopez, A. J. Ma, S. Toderas, S. Levine, and K. Barmak, *Microsc. Microanal.* 29 supplement\_1, 1581 (2023).
- X. Xu, Z. Yu, W. Y. Chen, A. Chen, A. Motta, and X. Wang, J. Nucl. Mater. 588 (2024).
- K. Barmak, J. Kim, C. S. Kim, W. E. Archibald, G. S. Rohrer, A. D. Rollett, D. Kinderlehrer, S. Ta'Asan, H. Zhang, and D. J. Srolovitz, Scr. Mater. 54, 1059 (2006).
- H.J. Frost, and C.V. Thompson, Curr. Opin. Solid State Mater. Sci. 1, 361 (1996).
- R. Backofen, K. Barmak, K.E. Elder, and A. Voigt, *Acta Mater.* 64, 72 (2013).
- 83. H.J. Frost, C.V. Thompson, and D.T. Walton, *Acta Metall. Mater.* 38, 1455 (1990).
- 84. N. Siddique, S. Paheding, C.P. Elkin, and V. Devabhaktuni, *IEEE Access* 9, 82031 (2021).
- N. S. Punn and S. Agarwal, ACM Trans. Multimedia Comput. Commun. Appl. 16 (2020).
- O. Ronneberger, P. Fischer, and T. Brox, Lecture Notes in Computer Science (Including Subseries Lecture Notes in Artificial Intelligence and Lecture Notes in Bioinformatics) 9351, 234 (2015).
- C.H. Lee, A. Khan, D. Luo, T.P. Santos, C. Shi, B.E. Janicek, S. Kang, W. Zhu, N.A. Sobh, A. Schleife, B.K. Clark, and P.Y. Huang, *Nano Lett.* 20, 3369 (2020).
- S. H. Yang, W. Choi, B. W. Cho, F. O. T. Agyapong-Fordjour, S. Park, S. J. Yun, H. J. Kim, Y. K. Han, Y. H. Lee, K. K. Kim, and Y. M. Kim, Adv. Sci. 8 (2021).
- J. Madsen, P. Liu, J. Kling, J.B. Wagner, T.W. Hansen, O. Winther, and J. Schiøtz, Adv. Theory Simul. 1, 1800037 (2018)
- L. von Chamier, R. F. Laine, J. Jukkala, C. Spahn, D. Krentzel, E. Nehme, M. Lerche, S. Hernández-Pérez, P. K. Mattila, E. Karinou, S. Holden, A. C. Solak, A. Krull, T. O. Buchholz, M. L. Jones, L. A. Royer, C. Leterrier, Y. Shechtman, F. Jug, M. Heilemann, G. Jacquemet, and R. Henriques, Nat. Commun. 12, 1 (2021).
- X. Xu, Z. Yu, A. Motta, and X. Wang, *Microsc. Microanal*. 28, 2036 (2022).
- X. Gu, X. Yang, W. Wang, Y. Jin, and D. Meng, in Proceedings—2012 IEEE 7th International Conference on Networking, Architecture and Storage, NAS 2012 (2012), pp. 94–98.
- J. Na, J. Lee, S.-H. Kang, S.-J. Kim, and S. Lee, *Mater Charact* 206, 1044 (2023).
- M. Wittwer, B. Gaskey, and M. Seita, *Mater Charact* 174, 110978 (2021).
- F. J. Humphreys, G. S. Rohrer, and A. Rollett, Recrystallization and Related Annealing Phenomena (Third Edition) (2017).
- B. Conry, M. Kole, W. R. Burnett, J. B. Harley, M. R. Tonks, M. S. Kesler, and A. R. Krause, J. Am. Ceram. Soc. 1 (2023).

- 97. S.J. Dillon, and G.S. Rohrer, Acta Mater. 57, 1 (2009).
- 98. C. Goux, Can. Metall. Q. 13, 9 (1974).
- E. R. Homer, S. Patala, and J. L. Priedeman, Sci. Rep. 5, 1 (2015).
- 100. V. Randle, Mater. Sci. Technol. 26, 774 (2010).
- Y. Pang, and P. Wynblatt, J. Am. Ceram. Soc. 88, 2286 (2005).
- S. Kobayashi, T. Yoshimura, S. Tsurekawa, T. Watanabe, and J. Cui, *Mater. Trans.* 44, 1469 (2003).
- N. Shibata, F. Oba, T. Yamamoto, and Y. Ikuhara, *Philos. Mag.* 84, 2381 (2004).
- P. Lin, G. Palumbo, U. Erb, and K.T. Aust, Scripta Met Mater 33, 1387 (1995).
- 105. L.C. Lim, and T. Watanabe, Scripta Met 23, 489 (1989).
- S. Kobayashi, A. Kamata, and T. Watanabe, Scripta Mater. 61, 1032 (2009).
- 107. T. Watanabe, J. Mater. Sci. 46, 4095 (2011).
- 108. M. Wagih, and C.A. Schuh, Scr. Mater. 237, 115716 (2023).
- 109. J. Zhang, W. Ludwig, Y. Zhang, H.H.B. Sørensen, D.J. Rowenhorst, A. Yamanaka, P.W. Voorhees, and H.F. Poulsen, Acta Mater. 191, 211 (2020).
- S. Ratanaphan, Y. Yoon, and G. S. Rohrer, J. Mater. Sci. 49 (2014).
- W. Zhu, G. Wu, A. Godfrey, S. Schmidt, Q. He, Z. Feng, T. Huang, L. Zhang, and X. Huang, Scr. Mater. 214, 114677 (2022).
- H. Beladi, N.T. Nuhfer, and G.S. Rohrer, *Acta Mater.* 70, 281 (2014).
- D.M. Saylor, A. Morawiec, and G.S. Rohrer, *Acta Mater*. 51, 3663 (2003).
- O. Chirayutthanasak, R. Sarochawikasit, S. Khongpia, T. Okita, S. Dangtip, G.S. Rohrer, and S. Ratanaphan, Scr. Mater. 240, 115821 (2024).
- A.D. Darbal, K.J. Ganesh, X. Liu, S.B. Lee, J. Ledonne, T. Sun, B. Yao, A.P. Warren, G.S. Rohrer, A.D. Rollett, P.J. Ferreira, K.R. Coffey, and K. Barmak, *Microsc. Microanal*. 19, 111 (2013).
- A. King, M. Herbig, W. Ludwig, P. Reischig, E.M. Lauridsen, T. Marrow, and J.Y. Buffière, Nucl Instrum Methods Phys Res B 268, 291 (2010).
- 117. D.J. Jensen, and H.F. Poulsen, Mater Charact 72, 1 (2012).
- 118. "Transmission Kikuchi Diffraction" (Oxford Instruments, n.d.). https://www.ebsd.com/ebsd-techniques/transmission-kikuchi-diffraction. Accessed 29 Nov 2023.
- X. Liu, N. T. Nuhfer, A. P. Warren, K. R. Coffey, G. S. Rohrer, and K. Barmak (2015).
- X. Liu, A.P. Warren, N.T. Nuhfer, A.D. Rollett, K.R. Coffey, and K. Barmak, Acta Mater. 79, 138 (2014).
- J. Gruber, H.M. Miller, T.D. Hoffmann, G.S. Rohrer, and A.D. Rollett, Acta Mater. 57, 6102 (2009).
- 122. J. Gruber, A.D. Rollett, and G.S. Rohrer, *Acta Mater.* 58, 14 (2010).
- J. Gruber, D.C. George, A.P. Kuprat, G.S. Rohrer, and A.D. Rollett, Scr. Mater. 53, 351 (2005).
- 124. M.J. Patrick, G.S. Rohrer, O. Chirayutthanasak, S. Ratanaphan, E.R. Homer, G.L.W. Hart, Y. Epshteyn, and K. Barmak, Acta Mater. 242, 118476 (2023).
- O. Chirayutthanasak, R. Sarochawikasit, A. Wisitsorasak, N. Rujisamphan, T. Frolov, T. Oppelstrup, S. Dangtip, G. S. Rohrer, and S. Ratanaphan, Scr. Mater. 209 (2022).
- S. Ratanaphan, T. Boonkird, R. Sarochawikasit, H. Beladi,
   K. Barmak, and G.S. Rohrer, Mater. Lett. 186, 116 (2017).
- V.V. Bulatov, B.W. Reed, and M. Kumar, *Acta Mater*. 65, 161 (2014).
- 128. E. R. Homer, G. L. W. Hart, C. Braxton Owens, D. M. Hensley, J. C. Spendlove, and L. H. Serafin, *Acta Mater*. 234 (2022).
- M. Ohring, Materials Science of Thin Films (Elsevier, 2002).
- L.I. Maissel, R. Glang, and P.P. Budenstein, J. Electrochem. Soc. 118, 114C (1971).
- J.K. Mackenzie, and J.F. Nicholas, J. Phys. Chem. Solids 23, 197 (1962).

- J.K. Mackenzie, A.J.W. Moore, and J.F. Nicholas, J. Phys. Chem. Solids 23, 185 (1962).
- R. Carel, C.V. Thompson, and H.J. Frost, *Acta Mater.* 44, 2479 (1996).
- C.C. Wong, H.I. Smith, and C.V. Thompson, Appl. Phys. Lett. 48, 335 (1986).
- 135. C.V. Thompson, Scr. Metall. Mater. 28, 167 (1993).
- 136. D.W. Hoffman, and J.W. Cahn, Surf. Sci. 31, 368 (1972).
- 137. J. l. Cahn and D. L. Hoffman, Acta Metall. 22, 1205 (1974).
- 138. D.M. Saylor, and G.S. Rohrer, *Interface Sci.* 9, 35 (2001).
- D.J. Rowenhorst, and P.W. Voorhees, Metall. Mater. Trans. A Phys. Metall. Mater. Sci. 36, 2127 (2005).
- 140. A. Moraweic, Acta Mater. 48 (2000).
- Y.-F. Shen, X. Zhong, H. Liu, R.M. Suter, A. Morawiec, and G.S. Rohrer, *Acta Mater.* 166, 126 (2019).
- 142. H. Beladi and G. S. Rohrer, Acta Mater. 61 (2013).
- D.M. Saylor, A. Morawiec, and G.S. Rohrer, *Acta Mater*. 51, 3675 (2003).
- E.A. Holm, G.S. Rohrer, S.M. Foiles, A.D. Rollett, H.M. Miller, and D.L. Olmsted, Acta Mater. 59, 5250 (2011).
- S.J. Dillon, Y.F. Shen, and G.S. Rohrer, J. Am. Ceram. Soc. 105, 2925 (2022).
- G.S. Rohrer, E.A. Holm, A.D. Rollett, S.M. Foiles, J. Li, and D.L. Olmsted, *Acta Mater.* 58, 5063 (2010).
- D.M. Saylor, A. Morawiec, and G.S. Rohrer, *J. Am. Ceram. Soc.* 85, 3081 (2002).
- 148. C. Ophus, Microsc. Microanal. 25, 563 (2019).
- C.S. Nichols, C.M. Mansuri, S.J. Townsend, and D.A. Smith, Acta Metall. Mater. 41, 1861 (1993).
- F.M. Ross, and A.M. Minor, In Situ Transmission Electron Microscopy (Springer, New York, 2019), pp101–187.
- Z. Ma, L. Niu, W. Jiang, S. Malunavar, X. Wang, and B. D. A. Levin, *J. Phys.: Mater.* 4, 042005 (2021).
- S. Simoes, R. Calinas, M.T. Vieira, M.F. Vieira, and P.J. Ferreira, Nanotechnology 21, 145701 (2010).
- 153. C. Ding, W. Chen, S. Sabbaghianrad, J. Xu, D. Shan, B. Guo, and T.G. Langdon, *Mater Charact* 173, 110929 (2021).
- S. Kumar, T. Alam, and A. Haque, MRS Commun 3, 101 (2013).
- S. Stangebye, Y. Zhang, S. Gupta, E. Hosseinian, F. Yu, C. Barr, K. Hattar, O. Pierron, T. Zhu, and J. Kacher, *Materialia (Oxford)* 16 (2021).
- C.V. Thompson, and R. Carel, J. Mech. Phys. Solids 44, 657 (1996).
- J. Wei, B. Feng, R. Ishikawa, T. Yokoi, K. Matsunaga, N. Shibata, and Y. Ikuhara, Nat. Mater. 20, 951 (2021).

- C.M. Barr, E.Y. Chen, J.E. Nathaniel, P. Lu, D.P. Adams, R. Dingreville, B.L. Boyce, K. Hattar, and D.L. Medlin, Sci. Adv. 8, 900 (2022).
- K.L. Merkle, L.J. Thompson, and F. Phillipp, *Interface Sci.* 12, 277 (2004).
- 160. Q. Zhu, G. Cao, J. Wang, C. Deng, J. Li, Z. Zhang, and S. X. Mao, Nat. Commun. 10, 1 (2019).
- Q.Z. Hong, K. Barmak, and L.A. Clevenger, J. Appl. Phys. 72, 3423 (1992).
- Q.Z. Hong, K. Barmak, S.Q. Hong, and L.A. Clevenger, J. Appl. Phys. 74, 4958 (1993).
- 163. D. Dzhigaev, Y. Smirnov, P. A. Repecaud, L. A. B. Marçal, G. Fevola, D. Sheyfer, Q. Jeangros, W. Cha, R. Harder, A. Mikkelsen, J. Wallentin, M. Morales-Masis, and M. E. Stuckelberger, Commun. Mater. 3, 1 (2022).
- Z. Yu, X. Xu, W.Y. Chen, Y. Sharma, X. Wang, A. Chen, C.J. Ulmer, and A.T. Motta, *Acta Mater.* 231, 117856 (2022).
- Y. Bi, Y. Tian, M. Xu, E. Boltynjuk, L.V. Estrada, H. Hahn, J. Han, D.J. Srolovitz, and X. Pan, *Microsc. Microanal.* 29, 1509 (2023).
- M.P. Anderson, D.J. Srolovitz, G.S. Grest, and P.S. Sahni, Acta Metall. 32, 783 (1984).
- C.J. Marvel, C. Riedel, W.E. Frazier, A.D. Rollett, J.M. Rickman, and M.P. Harmer, Acta Mater. 239, 118262 (2022).
- 168. L.Q. Chen, Annu. Rev. Mater. Res. 32, 113 (2003).
- P. J. Diggle, Statistical Analysis of Spatial and Spatio-Temporal Point Patterns, Third Edition 1 (2013).
- 170. J. M. Rickman, K. Barmak, Y. Epshteyn, and C. Liu, *Npj Comput. Mater.* **9**, 1 (2023).
- P. Vedanti, X. Wu, and V. Berdichevsky, Sci. Rep. 10, 1 (2020).
- J. M. Rickman, K. Barmak, B. Y. Chen, and M. Patrick, Sci. Rep. 13, 1 (2023).

**Publisher's Note** Springer Nature remains neutral with regard to jurisdictional claims in published maps and institutional affiliations.

Springer Nature or its licensor (e.g. a society or other partner) holds exclusive rights to this article under a publishing agreement with the author(s) or other rightsholder(s); author self-archiving of the accepted manuscript version of this article is solely governed by the terms of such publishing agreement and applicable law.